Polymer Journal (2011) 43, 583–593

www.nature.com/pj

INVITED REVIEW

# Development and applications of polyolefin– and rubber–clay nanocomposites

Makoto Kato, Arimitsu Usuki, Naoki Hasegawa, Hirotaka Okamoto and Masaya Kawasumi

**A nylon 6-clay hybrid (nanocomposite, NCH) was developed by Toyota CRDL group. In the NCH, the silicate layers of clay mineral are dispersed on a nanometer level and are strongly interacted with the matrix, and then significant improvements in the mechanical properties of the material or the discovery of unexpected new properties were realized. Polypropylene (PP) is the most widely used polymer, and then an appearance of a PP–clay nanocomposite has been desired for a long time. As a PP does not include any polar groups in its backbone, it was thought that the homogeneous dispersion of the silicate layers would not be realized. But we have developed successfully PP–clay nanocomposite using organoclay and modified PP. That is, organophilic clay, PP oligomer carrying polar groups and PP were melt-blended. This is a direct polymer intercalation process for preparing polymer nanocomposites by melt compounding, a useful process from an industrial standpoint. We have also developed successfully other polyolefin polymers (polyethylene), polyolefin rubbers (ethylene–propylene elastomer, ethylene–propylene diene monomer) and nanocomposites by this direct polymer intercalation process or by techniques based on direct polymer intercalation process. These prepared polyolefin nanocomposites exhibit superior mechanical, thermal and gas barrier properties.**
*Polymer Journal* (2011) **43,** 583–593; doi:10.1038/pj.2011.44; published online 1 June 2011

**Keywords:** clay mineral; nanocomposite; polyolefin; polyolefin rubber

## INTRODUCTION

A nylon 6-clay hybrid (nanocomposite, NCH) has been developed, in which the silicate layers of clay mineral are dispersed on a nanometer level and strongly interact with the matrix.[1–3] Significant improvements in the mechanical properties of the material and the discovery of new properties also have been realized. Polyolefins (such as polypropylene (PP) and polyethylene (PE)) are the most widely used polymers, and there has been interest in the development of a polyolefin–clay nanocomposite. As polyolefins do not include any polar groups in the backbone, a homogeneous dispersion of silicate layers did not seem to be possible. However, the successful development of a PP–clay nanocomposite using organoclay and modified PP has been achieved. Nanocomposites of clay with various polyolefin polymers and rubbers have been developed. This report provides an overview of preparation methods and properties of polyolefin polymer/rubbers–clay nanocomposites.

Montmorillonite (MMT) was used as the clay mineral in this investigation of polyolefin–clay nanocomposites. MMT composed of micro-sized particles formed from stacks of three-layer 'sandwiches' is most widely used. In these sandwiches, a tetrahedral sheet of silicon oxide is on both sides of a central octahedral sheet of aluminum oxide (a 2:1.clay). The plate-shaped layers are 0.96-nm thick and have an average diameter of about 100–500 nm, which represents filler with a significantly large aspect ratio. For comparison, a glass fiber of 13 μm in diameter with a length of 0.3 mm would be $4\times10^9$ times the size of a typical plate-shaped layer. In other words, if the same volumes of glass fiber and silicate were evenly dispersed, there would be roughly $10^9$ times more fiber than layers. Furthermore, the specific surface area available would increase exponentially. These properties of size and surface provide reinforcement equal to that of glass fiber in a small amount of MMT. The chemical formula of MMT is $(Na, Ca)_{0.33}(Al, Mg)_2(Si_4O_{10})(OH)_2{\cdot}nH_2O$. The central aluminum located between the plate-shaped layers is partially substituted with $Mg^{2+}$, $Na^+$ and $Ca^+$ ions that are exchangeable with organic ions, such as ammonium, phosphonium and sulfonium, giving the MMT cation-exchange capabilities. Ammonium ions (primary, secondary, tertiary or quaternary) are easy to obtain and thus are usually used as organic modifiers. MMT becomes compatible with organic materials by treatment with an organic modifier, and MMT treated with an organic modifier is called organo-MMT.

## PP–CLAY NANOCOMPOSITE

### Oligomer with polar group intercalation

In 1997, a polyolefin polymer (oligomer) with hydroxyl groups that can be intercalated into MMT was reported.[4] The polyolefin backbone is PE, with hydroxyl groups (Polytel H, Mitsubishi Chemical, Tokyo, Japan) on both ends intercalated between silicate layers of MMT ion-exchanged with dimethyl dioctadecyl ammonium ions (2C18-MMT).

Coating Laboratory, Toyota Central Research and Development Laboratories, Inc., Nagakute_cho, Japan
Correspondence: Dr M Kato, Coating Laboratory, Toyota Central Research and Development Laboratories, Inc, 41-1 Yokomichi, Nagakute_cho 4801192, Japan.
E-mail: makoto@mosk.tytlabs.co.jp
Received 8 February 2011; revised 20 April 2011; accepted 21 April 2011; published online 1 June 2011

### Preparation of PP oligomer–clay nanocomposites

On the basis of the discovery of intercalation of polyolefin oligomers with hydroxyl groups, a maleic anhydride-modified polypropylene (MA-g-PP) was intercalated into MMT by melt compounding.[5,6] By changing the ratio of MA-g-PP to organo-MMT treated with octadecyl ammonium ions (C18-MMT), the effect of MA-g-PP on swelling of C18-MMT was examined. The state of swelling was verified by X-ray diffraction measurements. Figure 1 shows X-ray diffraction patterns of the C18-MMT/MA-g-PP nanocomposites mixed in various proportions. When MA-g-PP was added in amounts greater than three times the amount of C18-MMT, the sharp peaks that showed a layered structure disappeared as the proportion of MA-g-PP increased. These results indicate that MA-g-PP is intercalated between the layers of C18-MMT and the silicate layers are dispersed uniformly in the MA-g-PP matrix. The PP oligomers with one polar group (for example, carboxy and hydroxyl groups) per ~25 U of PP also were found to be intercalated between the layers of organoclay.

Figure 2 shows a schematic diagram of the silicate layers of the MMT dispersing process in MA-g-PP. When PP, without a polar group, and C18-MMT were melt-blended, intercalation did not occur. However, MA-g-PP then intercalated between the layers of C18-MMT due to strong hydrogen bonding between the maleic anhydride groups and the polar silicate surface. As the ratio of modified PP increased, more modified PPs were intercalated between the layers of organic clay until exfoliation occurred.

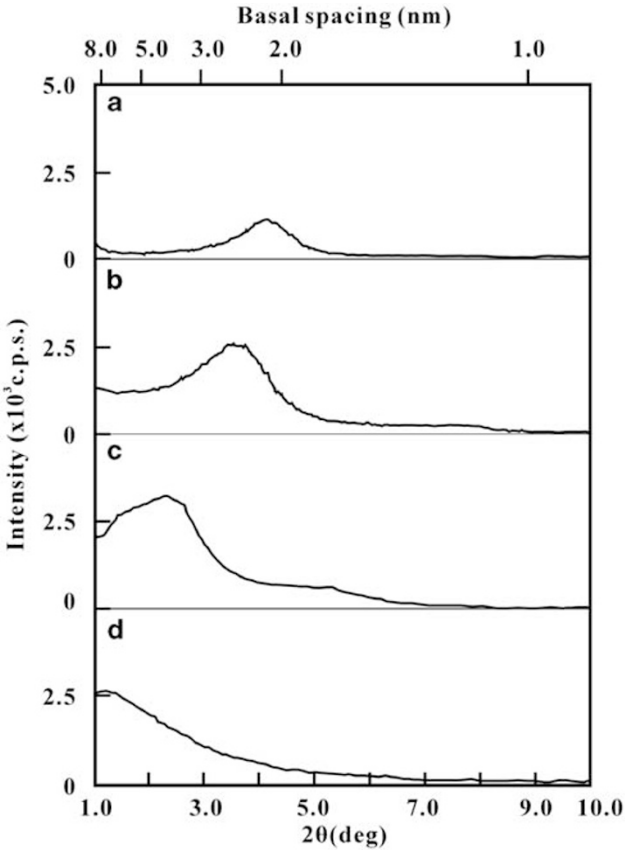


**Figure 1** X-ray diffraction patterns of C18-MMT/MA-g-PP nanocomposites mixed in various proportions. MA-g-PP, maleic anhydride-modified polypropylene; MMT, montmorillonite. **(a)** C18-MMT, **(b)** C18-MMT/MA-g-PP=3/1 by weight, **(c)** C18-MMT/MA-g-PP=1/1 and **(d)** C18-MMT/MA-g-PP=1/3.

### Mechanical properties of polypropylene–clay nanocomposites using modified polypropylene

The mechanical properties of PP–clay nanocomposite prepared by melt blending with MA-g-PP and C18-MMT were investigated.[6,7] Table 1 shows the tensile properties of the PP–clay nanocomposites (PPCNs) and related compounds. PPCN is prepared by melt blending with MA-g-PP and C18-MMT. In this study, Exxelor PO 1015 (ExxonMobil Chemical, Houston, TX, USA) was used as MA-g-PP. The acid value of PO 1015 is 2.1 mg KOH per g. This acid value corresponded to 0.2 wt% of the amount of maleic acid in the PP. The weight-average molecular weight of PO 1015 is 209 000. PPTC represents PP talc composite prepared by melt blending with MA-g-PP and talc (JR37, Japan Talc, Osaka, Japan). Talc was dispersed at a sub-micron level in PPTC. PP represents homo-PP, which was MA2 (Japan Polypropylene, Tokyo, Japan) PPCC represents PP–clay composite prepared by melt blending with PP and C18-MMT.

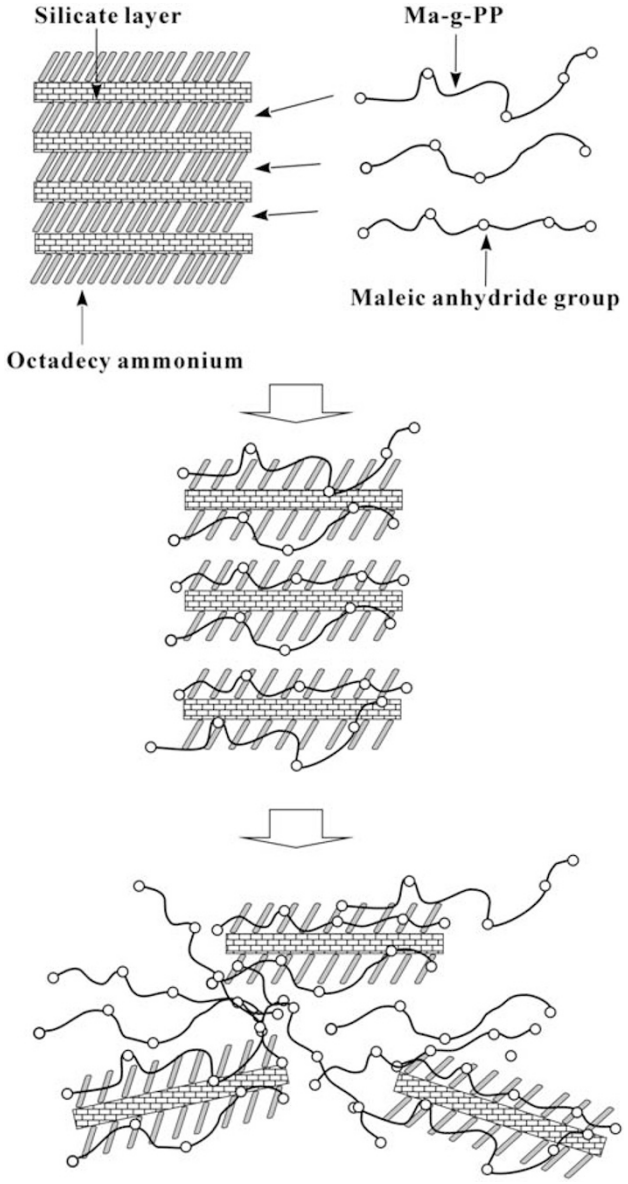


**Figure 2** Schematic representation of the intercalation process of C18-MMT and maleic anhydride-modified PP. MMT, montmorillonite; PP, polypropylene.

Figure 3 shows the relation between the tensile properties and amount of inorganic material in the samples. Figure 3a shows the tensile modulus and Figure 3b shows the tensile strength at the yield point. The tensile modulus increased with the amount of MMT added. Addition of 5.3 wt% MMT doubled the tensile modulus. The tensile strength also increased with the amount of MMT and tended to become saturated by the addition of 2 wt% of MMT. On addition of 5.3 wt% MMT, the tensile strength increased 1.2-fold. The tensile modulus and strength of the PPCN increased significantly compared with PPTC, in which talc was dispersed at a sub-micron level. When 4.4 wt% of MMT was added, the tensile modulus of PPCC with dispersed clays larger than sub-micron in size was 1.06 times greater than that of neat PP(MA2). The tensile strength of this PPCC was similar to that of MA2. The reinforcement effect in PPCN with dispersed nanometer-size silicate layers of MMT was much greater than that in PPTC and PPCC, in which the dispersed particulates were sub-micron size. This can be explained by a dispersion of nanometer-sized particles that increase the area of the interface with the matrix polymer, and therefore strengthen the interaction of the polymer chains with the particles. In contrast, the elongation at break of the PPCN decreased with an increase in the amount of added MMT. If the amount of added clay was $<3$ wt%, the elongation was $>200$%, and ductile behavior was observed. At 4 wt%, the elongation decreased to 23%. At 5 wt%, the breakage of PPCN MMT occurred by brittle fracture occurred without the manifestation of a yield point.

**Table 1 Tensile properties of PP–clay nanocomposites based on modified polypropylene and C18-MMT and related samples**

| | | | *Tensile properties* | | |
|---|---|---|---|---|---|
| *Sample* | *Type of inorganic* | *Inorganic content (wt%)* | *Modulus (MPa)* | *Strength (MPa)* | *Elongation at break (%)* |
| PO1015 | — | 0 | 429 | 21.1 | >200 |
| PPCN-2 | MMT | 2.1 | 578 (1.35) | 23.2 (1.10) | >200 |
| PPCN-3 | MMT | 2.8 | 639 (1.49) | 24.0 (1.14) | >200 |
| PPCN-4 | MMT | 3.8 | 707 (1.65) | 24.7 (1.17) | 23.1 |
| PPCN-5 | MMT | 5.3 | 797 (1.86) | 24.9 (1.18) | 10.5 |
| PPTC-2 | Talc | 1.9 | 489 (1.13) | 22.5 (1.07) | >200 |
| PPTC-5 | Talc | 5.0 | 546 (1.27) | 22.9 (1.09) | >200 |
| MA2 | — | 0 | 780 | 32.5 | >200 |
| PPCC | Montmorillonite | 4.4 | 830 (1.06) | 31.9 (0.98) | 105 |

Abbreviations: MA, maleic anhydride; MMT, montmorillonite; PP, polypropylene; PPCC, PP–clay composite; PPCN, PP–clay nanocomposite.
The values in parentheses are the relative value of the composites to those of the matrix polymer, respectively.
Head speed: 5 mm min$^{-1}$.

Figure 4 shows the change in dynamic storage moduli of PPCNs with temperature. Figure 4b shows relative values of the dynamic storage modulus of PO 1015, which is a matrix polymer. The storage moduli of the PPCNs were larger than that of PO 1015 over the entire temperature range ($-50$ to 130 °C), and increased with the amount of MMT. The relative values of the storage moduli of PPCNs compared with PO 1015 increased remarkably with temperature—they were larger than the glass transition temperature ($Tg$) value of PP, and reached a maximum value at around 60 °C. The dynamic storage modulus of PPCN-5 was 1.5 times larger than that of PO 1015 at $-50$ °C, 2.0 times larger at 30 °C, 2.3 times larger at 60 °C and 2.0

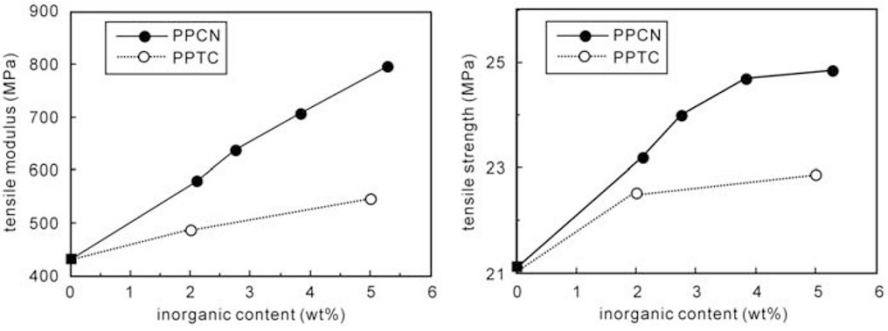


**Figure 3** Relation between tensile modulus, tensile strength and amount of clay. PPCN, polypropylene–clay nanocomposite; PPTC, polypropylene talc.

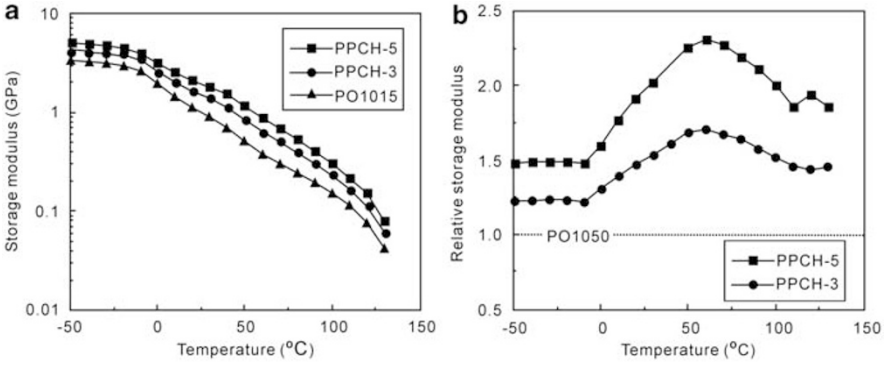


**Figure 4** Dynamic viscoelastic measurements for PPCN and PO 1015: (**a**) storage modulus, (**b**) relative storage modulus of PPCN to PO 1015. PPCN, polypropylene–clay nanocomposite.

times larger at 100 °C. The *Tg* did not change, even on addition of more MMT.

Figure 5 shows the dynamic storage modulus and relative storage modulus of PPTC-5, which contains talc. With PPTC-5, the reinforcement effect increased at temperatures greater than the *Tg*. However, reinforcement increased only by 1.5 times, a small increase compared with PPCN. In addition, PPTC-5 did not exhibit a maximum value when the temperature was increased. Figure 6 shows the storage modulus of PPCC and the relative storage modulus of PPCC compared with MA2. Although the reinforcement effect of PPCC increased at a temperature greater than the *Tg*, the increase in reinforcement effect was small at 1.2–1.3 times. PPCC also did not exhibit a maximum value when the temperature was increased.

**Preparation and characterization of a polypropylene–clay nanocomposite using MA-g-PP as a compatibilizer**

Inorganic material is often dispersed into a polymer matrix using a compatibilizer. When MA-g-PP is used as a compatibilizer to disperse MMT into a PP matrix, PP nanocomposite is obtained easily. The MA-g-PP covers the hydrophilic surface of the silicate layer of MMT and stabilizes the interface between the silicate layer and PP matrix.

Two important factors affect the dispersibility and the physical properties of a PPCN when using modified PP (that is, MA-g-PP) as a compatibilizer:

1. Compatibility of the PP with the modified PP.
2. The type of clay.

Studies have demonstrated the importance of these factors using two types of MA-g-PP (U1001 and U1010, Sanyo Chemical Industries, Kyoto, Japan) and two types of organoclay (montmorillonite (C18-MMT) exchanged with octadecylammonium ions and synthetic mica (C18-MICA; Coop Chemical, Tokyo, Japan)).[8] MA2 (Japan Polypro, Tokyo, Japan) was used as the PP. The U1001 contains 2.3 wt% maleic anhydride, has a softening temperature of 154 °C, and has a molecular weight of 40 000. In contrast, U1010 contains 4.5 wt% maleic anhydride, and has a softening temperature of 145 °C and a molecular weight of 30 000. The properties of synthetic mica are similar to those of MMT. But the hydroxyl group of the edge of the silicate layer of synthetic mica is substituted by fluorine, making the synthetic mica slightly more hydrophobic than MMT.

**Compatibility between modified polypropylene and polypropylene and effects of clay types on dispersibility of the silicate layer**

The compatibility between PP and MA-g-PP is thought to be affected by the maleic anhydride groups in the modified PP, because the hydrophilicity of MA-g-PP is determined by the number of maleic anhydride groups. PPCN were prepared using two types of MA-g-PP (each with a different number of maleic anhydride groups) as compatibilizers.[8] The dispersibility of the silicate layers within these nanocomposites and their physical properties were determined. The effect of the method used to mix the PP, MA-g-PP and organoclay on the physical properties of the products was also examined.

Figure 6 shows photographs of MA2/U1010 (ca 80/20 by weight) and MA2/U1001 (ca 80/20) in a molten state at 200 °C as observed

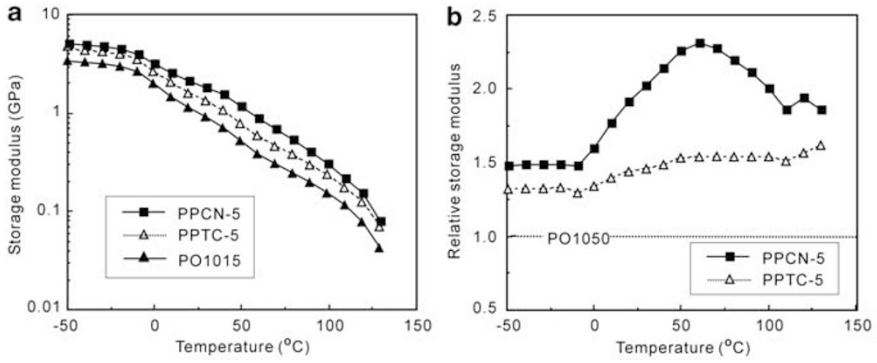


**Figure 5** Dynamic viscoelastic measurements for PPCN-5, PPTC-5 and PO 1015: (**a**) storage modulus, (**b**) relative storage modulus of PPCN-5 and PPTC-t to PO 1055. PPCN, polypropylene–clay nanocomposite; PPTC, polypropylene talc.

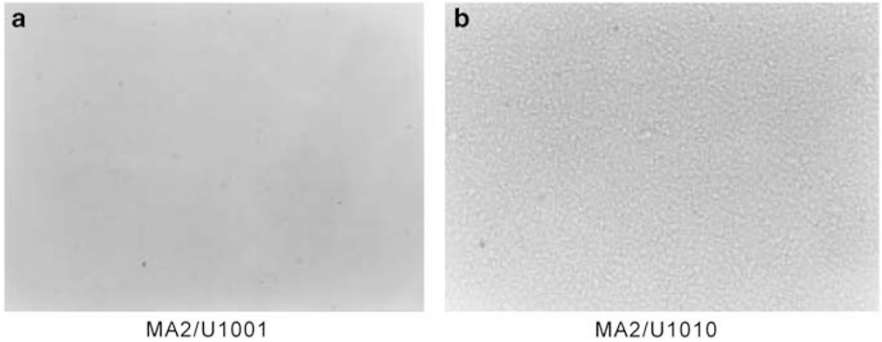


**Figure 6** Optical polarized micrographs of blends of PP with PP-MAs at their melt states (200 °C): (**a**) PP/1010 and (**b**) PP/1001. PPCN, polypropylene–clay nanocomposite; PPTC, polypropylene talc.

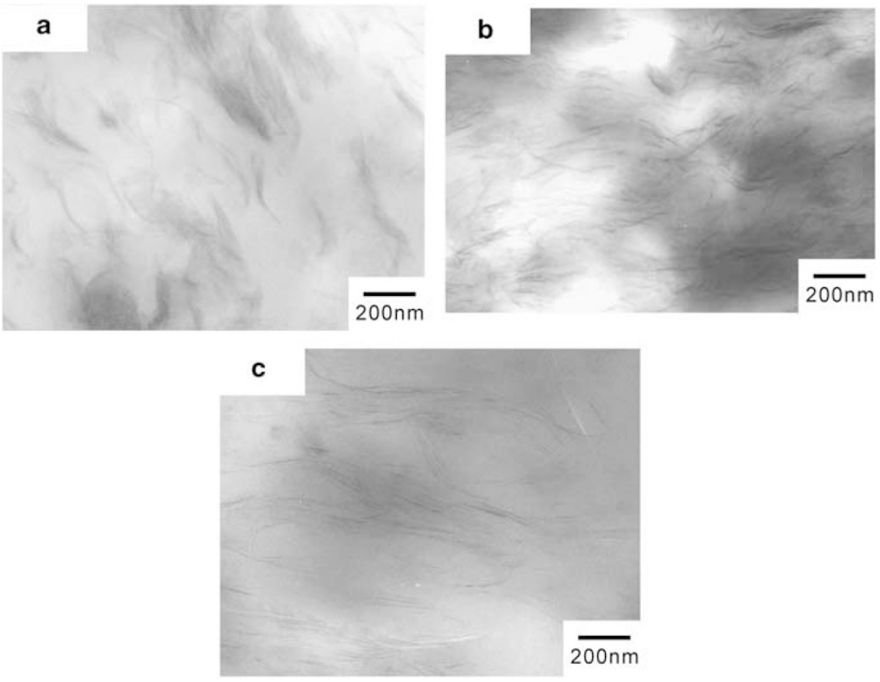


**Figure 7** Transmission electron micrographs of the PPCNs: (**a**) PPCN-C18-MMT/1001, (**b**) PPCN-C18-MMT/1010, (**c**) PPCN-C18-MICA/1001. MMT, montmorillonite; PPCN, polypropylene–clay nanocomposite; PPTC, polypropylene talc.

under an optical microscope. In the MA2/U1001 mixture, macroscopic phase separation was not observed by visual and optical methods. In contrast, non-uniformity was observed in the MA2/U1010 mixture. These results indicate that compatibility is better in the MA2/U1001 system than in the MA2/U1010 system. U1010 contains 4.5 wt% maleic anhydride groups, whereas U1001 contains only 2.3 wt%. The U1001 is more hydrophobic than U1001, thus, the compatibility with PP is higher for U1001.

Figure 7 shows transmission electron microscope images of the U1001-type PPCN (PP/U1001/C18-MMT=ca 70/20/7, Figure 7a) and U1010-type PPCN (PP/U1010/C18-MMT=ca 70/30/7, Figure 7b). Exfoliated silicate layers of MMT are dispersed more uniformly in the U1001-type PPCN than in the U1010-type PPCN. Many silicate layers with interlayer distances expanded to more than 5 nm (based on X-ray diffraction measurements) also were observed, indicating that the dispersibility of the silicate layers in the U1001-type PPCN is better than that in the U1010-type PPCN.

Figure 7c shows transmission electron microscope images of the U1001-type PPCN using C18-MICA, indicating that the dispersibility of the silicate layers was slightly better than that in the U1001-type PPCN using C18-MMT.

### Physical properties of PPCNs

Figure 8 shows the temperature dependence of the storage moduli, obtained from dynamic viscoelastic measurements of the U1010-type PPCN (PP/U1010/C18-MMT) and the U1001-type PPCN (PP/U1001/C18-MMT). Figure 8 presents the dependence of the type of MA-g-PP and the type of clay on the relative moduli of the PPCNs. All of the PPCNs exhibited similar relative moduli curves versus temperature. Below *T*g (obtained from tan $\delta$, ca 10 °C), the relative moduli were relatively small and were 1.3–1.4 times those of PP (Table 2). Above *T*g, they increased to 1.7–2.0 times those of PP (ca 50–80 °C) and then decreased to melt. Some differences in the relative moduli of the PPCNs were observed that depended on the type of

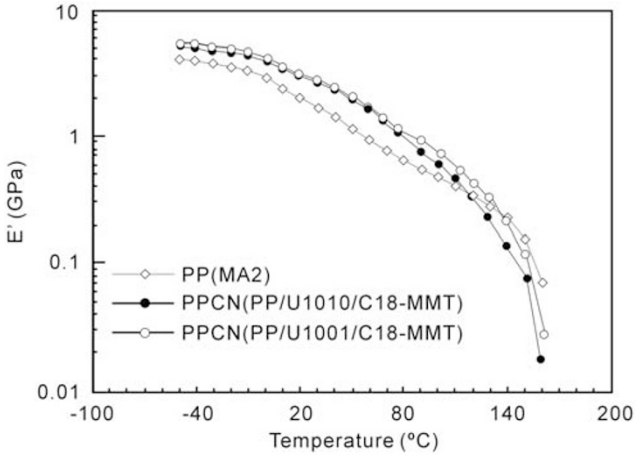


**Figure 8** Temperature dependence of the storage moduli of PPCN: PP/U1010/C18-MMT, PP/U1001/C18-MMT and PP(MA2). MMT, montmorillonite; PP, polypropylene; PPCN, PP–clay nanocomposite.

MA-g-PP and the type of clay. As seen from Figure 8, the relative moduli of the PPCNs using U1001 are greater than those of the PPCNs using U1010 at temperatures greater than 60 °C, regardless of the type of clay. This is probably due to the softening point of U1001 being higher than that of U1010 by 9 °C (Figure 9). Better dispersibility is another reason. In contrast, as seen from Table 2, the PPCNs using C18-MICA exhibited higher dynamic moduli compared with those of the PPCNs using C18-MMT, possibly due to the slightly better dispersibility of C18-MICA and the higher aspect ratio of synthetic mica compared with that of MMT.

### Possible dispersion mechanism

A possible dispersion mechanism of the clays in the PPCNs is proposed below. When PP and organoclay (C18-MICA or C18-

**Table 2 Dynamic storage moduli of PP–clay nanocomposites and related samples at various temperatures and their glass transition temperatures obtained from tan $\delta$**

| | Strage modulus[a] (GPa) | | | | |
|---|---|---|---|---|---|
| Sample | −40°C | 20°C | 80°C | 140°C | Tg[b] (°C) |
| PPCN-C18-MMT/1010 | 5.15 (1.31) | 3.12 (1.58) | 1.03 (1.59) | 0.13 (0.60) | 11 |
| PPCN-C18-MMT /1001 | 5.26 (1.34) | 3.09 (1.56 | 1.10 (1.70) | 0.21 (0.94) | 8 |
| PP/C18-MMT | 45.0 (1.15) | 2.36 (1.19) | 0.82 (1.26) | 0.28 (1.25) | 9 |
| PP/1010 | 3.92 (1.00) | 1.99 (1.01) | 0.60 (0.92) | 0.15 (0.68) | 13 |
| PP/1001 | 4.04 (1.03) | 2.02 (1.02) | 0.55 (0.85) | 0.14 (0.62) | 10 |
| PP | 3.92 | 1.98 | 0.65 | 0.22 | 13 |

Abbreviations: MMT, montmorillonite; PP, polypropylene.
[a]The values in parentheses are the relative values of the nanocomposites to those of PP.
[b]The glass transition temperatures were measured at the peak tops of tan $\delta$.

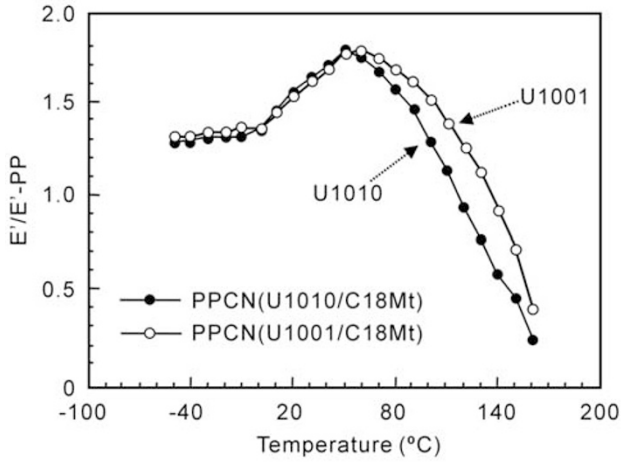


**Figure 9** Dependence of PP-MAs on relative dynamic storage moduli (E′/E′-PP) of the obtained PPCNs to that of PP as a function of temperature. MA, maleic anhydride; PP, polypropylene; PPCN, PP–clay nanocomposite.

MMT) were blended, no increase in the interlayer spacing of the organized clays was observed. Therefore, only the MA-g-PPs can intercalate into the silicate layers at the first stage of the melt mixing process. The driving force of the intercalation MA-g-PPs is the strong hydrogen bonding between the maleic anhydride group (or COOH group generated from hydrolysis of the maleic anhydride group) and the oxygen groups of the silicates. The interlayer spacing of the clay increases and the interaction of the layers should be weakened. The intercalated clays with the MA-g-PPs contact PP under a strong shear field. If the miscibility of PP-MA with PP is good enough for dispersion at the molecular level, exfoliation of the intercalated clay should occur smoothly. In contrast, if the miscibility is not good enough, phase separation occurs with no exfoliation. Therefore, not only the intercalation ability of the MA-g-PPs but also the miscibility is a very important factor to achieve exfoliated homogeneous dispersion of the clays using MA-g-PPs as a compatibilizer.

## PE–CLAY NANOCOMPOSITE

### Preparation and evaluation of the physical properties of a PE–clay nanocomposite

A PE–clay nanocomposite has been prepared by a method similar to that for preparing PP–clay nanocomposites.[9] The materials for preparing a PE–clay nanocomposite include PE, maleic anhydride-modified PE and C18-MMT. The PE used was KF380 (Japan Polyethylene, Tokyo, Japan). KF380 has a melt flow index of 4.0 g per 10 min (ASTM D1238 at 190 °C, 2.16 kg; PE). Maleic anhydride-modified PE was Fusabond 226D (E.I. DuPont, Wilmington, DE, USA). Fusabond 226D is a base resin linear low-density polyethylene (LLDPE), grafted maleic anhydride 0.90 wt%, and melt flow index 1.5 g per 10 min (ASTM D1238 at 190 °C, 2.16 kg; MA-g-PE).

Table 3 shows the composition of PE–clay nanocomposites and related samples. Table 4 shows the tensile properties and nitrogen gas permeability properties. Materials with high rigidity and high gas barrier properties were obtained. This gas barrier effect in the PE–clay nanocomposite can be explained by the formation of a torturous diffusion path resulting from the presence of dispersed silicate layers of clay, as in the case of NCH. Thus, the permeability coefficient of a gas traveling through the PE–clay nanocomposite can be analyzed using a geometrical model in which the silicate layers are dispersed. In films of PE–clay nanocomposites, silicate layers are aligned nearly parallel with the film surface. According to Nielsen,[10] the diffusion coefficient $D$ of a liquid or a gas can be calculated if the liquid or gas is in a composite material in which plate-like particles are in a planar orientation using the following equation:

$$D = D_0/\{1+(L/2d)V\}$$

**Table 3 Composition of prepared nanocomposites based on PE, MA-g-PE and C18-MMT**

| | | Composition (wt%) | | |
|---|---|---|---|---|
| Sample name | Clay | PE | MA-g-PE | Inorganic content (%) |
| PE | — | 100 | 0 | 0 |
| MA-g-PE | — | 0 | 100 | 0 |
| PE1 | — | 70 | 30 | 0 |
| PECN1 | C18-MMT | 70 | 30 | 5.4 |
| PECN2 | C18-MMT | 70 | 30 | 3.5 |
| PECN3 | C18-MMT | 0 | 100 | 5.2 |
| PECC | Na-MMT | 70 | 30 | 5.7 |

Abbreviations: MA-g-PE, maleic anhydride-modified polyethylene; MMT, montmorillonite; PE, polyethylene; PECC, polyethylene-clay composite.

**Table 4 Tensile properties and gas permeability coefficients of polyethylene–clay nanocomposite and related samples**

| | Tensile properties | | | | Gas permeability coefficient $\times 10^{13}$ |
|---|---|---|---|---|---|
| Sample name | Modulus (MPa) | Yield strength (MPa) | Yield strain (%) | Elongation at break (%) | ($cm^3$ (STP) cm $cm^{-2}$ $s^{-1}$ $Pa^{-1}$) |
| PE | 102 | 7.3 | 7.1 | >500 | 5.26 |
| MA-g-PE | 118 | 9.3 | 8.0 | 180 | 5.46 |
| PE1 | 99 | 7.5 | 7.7 | >500 | 5.32 |
| PECN1 | 180 (1.8) | 10.3 (1.4) | 5.6 | >500 | 3.78 |
| PECN2 | 140 (1.4) | 9.4 (1.3) | 6.8 | >500 | 3.91 |
| PECN3 | 157 (1.3) | 12.6 (1.4) | 7.0 | 155 | 3.48 |
| PECC | 103 (1.0) | 7.9 (1.1) | 8.4 | >500 | 5.48 |

Abbreviations: MA-g-PE, maleic anhydride-modified polyethylene; PE, polyethylene; PECC, polyethylene-clay composite.
Values in parentheses for the nanocomposites and PECC are relative to those of each matrix.

where $D_0$ is the diffusion coefficient in a matrix, $L$ is the size of one side of a plate-like particle, $d$ is the thickness and $V$ is the volume fraction of particles. When MMT is used at a level of 2%, $L$ is 100 nm, $d$ is 1 nm and $V$ is 0.0074, providing a $D/D_0$ value of 0.73. In the NCH, the calculated gas barrier effect $D/D_0$ is equivalent to the experimental value obtained for hydrogen (0.70) and water (0.63)[29]. In contrast, the calculated gas barrier effect $D/D_0$ is 0.5 in the PECN3, which is not equivalent to the experimental value obtained for nitrogen (0.64). The dispersibility of the silicate layer in PECN3 is not better than that in NCH.

## ETHYLENE PROPYLENE MONOMER (EPM)–CLAY NANOCOMPOSITE

### Preparation and characteristics of EPM–clay nanocomposites

EPM (M-class) rubber–clay nanocomposites (EPM-CNs) have been prepared by a melt intercalation method that contained different levels of octadecyl amine-modified clay (C18-MMT) and the characteristics of the nanocomposites reported.[11] The nanocomposites were prepared from maleic anhydride-modified EPM (MA-g-EPM) polymers containing 0.42 wt% maleic anhydride (4.81 mg KOH per g) with molecular weights of 125 000 and 397 000 as determined by gel permeation chromatography measurements.

The composition of EPM-CNs and related samples are summarized in Table 5. The composite materials of EPM and carbon or those of EPM and talc were prepared to compare the effect of reinforcement of MMT with that of the carbon black and the talc.

**Table 5 Composition and tensile properties of EPM–clay nanocomposites and related samples**

| *Sample* | *Filler* | *Inorganic content (wt%)* | *Modulus (MPa)* | *Strength at maximum (MPa)* | *Elongation at break (%)* |
|---|---|---|---|---|---|
| EPM-g-MA | — | 0 | 7.2 | 4.4 | 900 |
| EPM-CN 3 | C18-MMT | 2.9 | 11.2 | 3.7 | 550 |
| EPM-CN 6 | C18-MMT | 6.1 | 17.2 | 4.7 | 400 |
| EPM-CN 8 | C18-MMT | 8.3 | 23.2 | 4.2 | 130 |
| Composite 1 | Carbon black | 5 | 7.9 | 4.3 | 860 |
| Composite 2 | Carbon black | 15 | 12.8 | 4.2 | 600 |
| Composite 3 | Carbon black | 30 | 18.0 | 4.8 | 400 |
| Composite 4 | Talc | 4.9 | 7.1 | 3.6 | 820 |
| Composite 5 | Talc | 10.1 | 7.5 | 3.4 | 720 |

Abbreviations: EPM, ethylene propylene monomer; MA, maleic anhydride; MMT, montmorillonite.

### Dynamic storage moduli of EPM-CNs

Figure 10 shows the relation between the storage moduli and inorganic content of EPM-CNs and conventional composites at 20 and 80 °C. The storage modulus of EPM-CN 6 at 20 °C was comparable to the values for conventional composites with 30 wt% inorganic component loading (Figure 10a), indicating that the MMT dispersed at a nanometer level exhibits a fivefold greater reinforcement effect than carbon black or talc as conventional fillers. The EPM-CNs also showed an approximately fivefold greater reinforcement effect at 80 °C (Figure 10b).

### Creep properties of EPM-CNs

The creep properties were remarkably improved in EPM-CNs. Creep elongations of EPM-CNs were smaller compared with EPM-MA (Figure 11). The elongation of EPM-CN 6 was restricted to $<1\%$ at 30 h, whereas EPM-MA was elongated more than 50% at 1 h and then broke within 2 h. The composite with 5 wt% carbon black did not

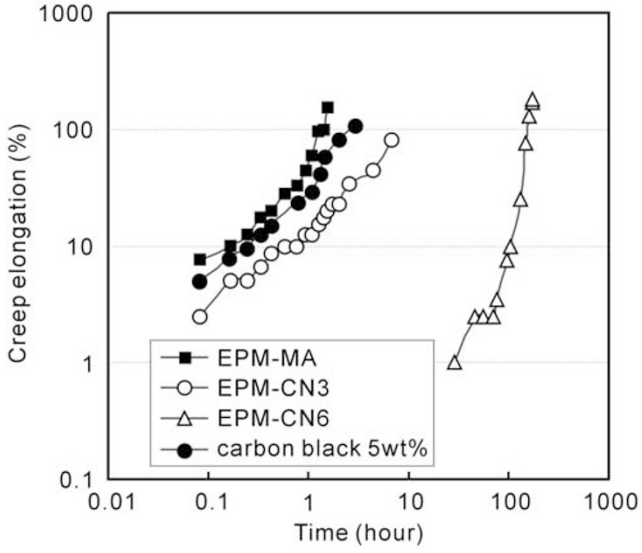


**Figure 11** Creep properties of ethylene propylene monomer–clay nanocomposite (EPM–CN) and related samples. MA, maleic anhydride.

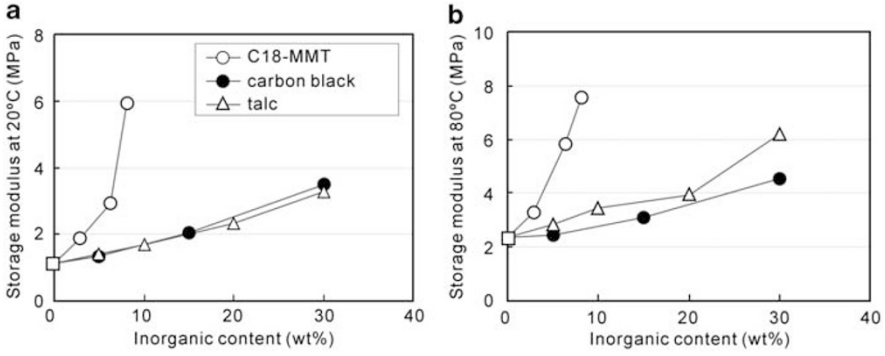


**Figure 10** Relation between storage moduli and inorganic content of ethylene propylene monomer–clay nanocomposites and those of conventional composites: (**a**) 20 °C and (**b**) 80 °C. MMT, montmorillonite.

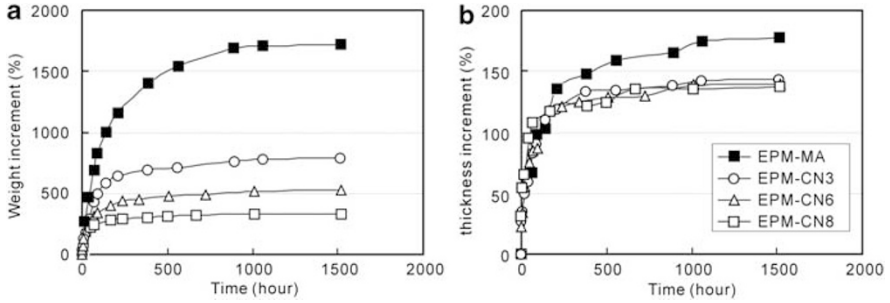


**Figure 12** Swelling properties of ethylene propylene monomer–clay nanocomposites (EPM-CNs) and EPM-MA in hexadecane: (**a**) by weight and (**b**) by thickness. MA, maleic anhydride.

exhibit any noticeable enhancement in creep resistance; it was elongated and broken within 3 h. The composite with 30 wt% carbon black showed enhancement in creep resistance nearly equal to that of EPM-CN 6. The maleic anhydride groups grafted to the EPM polymer chains were thought to be selectively adsorbed on the dispersed silicate layers and formed strong hydrogen bonding due to the affinity of maleic anhydrides for silicate layer surfaces. The silicate layers dispersed at the nanometer level were assumed to bridge with some polymer chains containing maleic anhydride groups. Thus, the dispersed silicate layers act like large pseudo-cross-link points and improve the creep resistance of EPM-CNs.

### Swelling properties of EPM-CNs

The swelling properties of EPM-CNs in hexadecane were studied and Figures 12a and b show the increments in weight and in sample thickness ($10\times10\times2\,mm^3$) soaked in hexadecane at 25 °C. The degree of swelling of EPM-CNs was dramatically restricted compared with EPM-MA. The weight increments of EPM-CNs decreased with increasing clay content and were also much smaller. The weight increment of EPM-MA was greater than 1700%, whereas that of EPM-CN 8 was limited to 333%. The length increments along the plane in EPM-CNs also become much smaller with increasing MMT content. In contrast, thickness increments were minimally restricted by MMT loading (Figure 12b). Not only the polymer chains but also the dispersed silicate layers at a nanometer level were orientated in parallel with a sheet plane prepared by compression molding. This orientation of both the silicate layers and the polymer chains is believed to selectively restrict the swelling increment along the length on the plane in EPM-CNs. Figure 13 shows the swelling increment (1500 h soak) in weight as a function of inorganic content for both EPM-CNs and conventional composites. The restricting effect on swelling by MMT is superior to that provided by conventional fillers. For example, the weight increment of EPM-CN 3 was approximately equal to that of the conventional composites with about a 20 wt% filler loading.

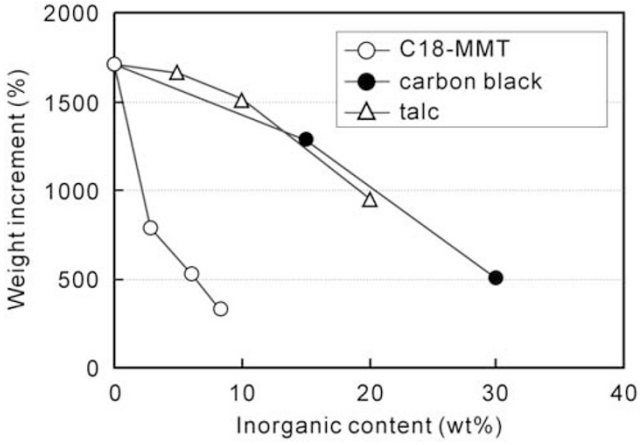


**Figure 13** Swelling increment in weight as a function of inorganic content: C18-MMT, carbon black, talc. MMT, montmorillonite.

## ETHYLENE PROPYLENE DIENE MONOMER (EPDM)–CLAY NANOCOMPOSITE

### Preparation of EPDM nanoclay composites using an *in situ* intercalation method

The extent of dispersion of the silicate layers of a clay (that is, MMT) in a PP–clay nanocomposite depends on the miscibility of the matrix and the compatibilizer. To enhance the fine dispersion state of silicate layers of clay, a modified polymer matrix with the same composition as the compatibilizer is needed. However, it is very difficult to modify EPDM rubbers because the crosslinking reaction has already been completed. Miscibility of the compatibilizer in a polymer matrix is also dependent on the amount of polar groups in the compatibilizer.

To address this issue, an EPDM–clay nanocomposite was prepared using an EPDM vulcanized with modifying accelerators.[12] Five types of vulcanization accelerators for this *in situ* modification were investigated: thiourea (ethylenethiourea, NPV/C), thiazole (2-mercaptobenzothiazole, M), sulfonamide (*N*-cyclohexyl-2-benzothiazylsulfenamide, CZ), thiuram (tetramethylthiuram monosulfide, TS) and dithiocarbamate (zinc dimethyldithiocarbamate, PZ). EPDM and a clay treated with octadecyl ammonium ($C_{18}H_{37}NH_3^+$) (C18-MMT) were mixed at 200 °C in a twin screw extruder. The blended material obtained, zinc oxide (5 p.h.r.), stearic acid (1 p.h.r.), sulfur (1.5 p.h.r.), and the vulcanization accelerator (1.5 p.h.r.) were compounded using a mixing roll. The vulcanized EPDM was then press molded at 160 °C for 30 min to yield EPDM–clay nanocomposites. The X-ray diffraction patterns of C18-MMT and EPDM–clay nanocomposites using the five types of vulcanization were examined. For the EPDM–clay nanocomposites prepared using NPV/C, M and CZ, a peak at a diffraction angle between 2° and 5° that clearly indicates the formation of an intercalation type of EPDM–clay nanocomposite in which the silicate layers of MMT are stacked was formed, but the interlayer distance is greater than that of C18-MMT. For TS and PZ, however, the peak generated by the orderly stacked layers of C18-MMT disappeared and the diffraction strength of the nanocomposite gradually shifted toward a lower angle. This diffraction pattern indicates the formation of the exfoliation type of EPDM–clay nanocomposite. The transmission

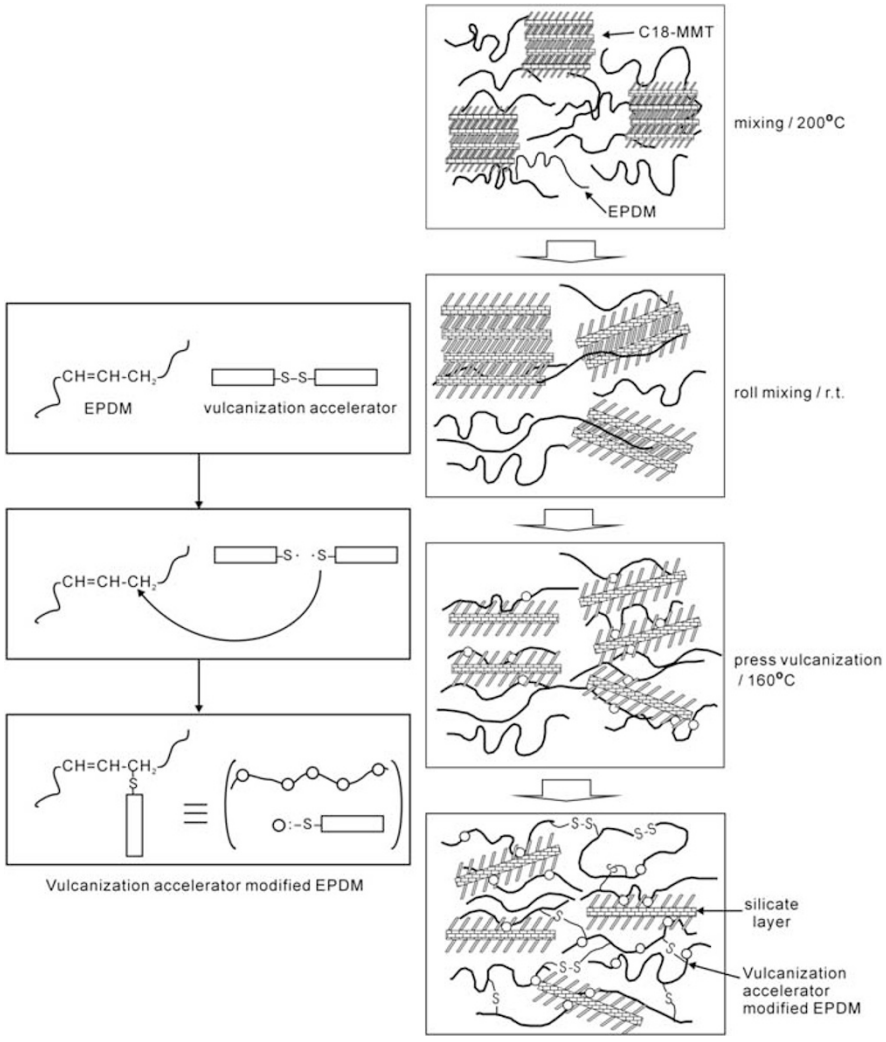


**Figure 14** Schematic representation of a proposed mechanism of ethylene propylene diene monomer (EPDM) intercalation into a clay gallery.

**Table 6 Properties of EPDM–clay nanocomposites with different vulcanization accelerators**

| *System* | *EPDM–clay nanocomposite (C18-Mt 7 p.h.r.)* | | | | | *EPDM* |
|---|---|---|---|---|---|---|
| *Vulcanization accelerator* | *NPV/C* | *M* | *PZ* | *CZ* | *TS* | *PZ* |
| *Properties* | | | | | | |
| Tensile strength (MPa) | 8.0 | 7.5 | 8.1 | 11.0 | 10.1 | 5.0 |
| Elongation at break (%) | 307 | 173 | 185 | 443 | 520 | 280 |
| 100% Tensile stress (MPa) | 1.9 | 1.8 | 1.7 | 2.3 | 2.3 | 1.6 |
| Storage modulus (MPa, 10 Hz, 25 °C) | 5.5 | 5.3 | 5.8 | 6.0 | 6.2 | 3.3 |
| $N_2$ permeability at 60 °C ($\times 10^{-9}$ cm$^3$ cm cm$^{-2}$ s$^{-1}$ cmHg$^{-1}$) | 1.8 | 2.2 | 2.1 | 1.7 | 1.7 | 2.4 |

Abbreviations: CZ, *N*-cyclohexyl-2-benzothiazylsulfenamide; EPDM, ethylene propylene diene monomer; M, 2-mercaptobenzothiazole; NPV/C. ethylenethiourea; PZ, zinc dimethyldithiocarbamate; TS, tetramethylthiuram monosulfide.

electron microscope image also indicated that the EPDM–clay nanocomposite using the PZ vulcanization accelerator was the exfoliation type of EPDM–clay nanocomposite.

A proposed mechanism of EPDM intercalation into a clay gallery is illustrated in Figure 14. The TS- and PZ-type vulcanization accelerators dissociate into radicals themselves during vulcanized process. The radicals combine with carbon atoms in the EPDM chains to polarize the EPDM molecules. These EPDM molecules intercalate into the clay galleries through hydrogen bonds between the polar substituents on the EPDM and the MMT surface. The properties of the exfoliation type nanocomposites obtained with the TS or PZ vulcanization accelerators were superior to those of the intercalation type nanocomposites that were obtained with the NPV/C, M and CZ accelerators. Tensile strength, elongation at break, tensile stress at 100% elongation, storage modulus and gas barrier properties of the exfoliation type nanocomposites were greater than those of the intercalation type (Table 6).

## CONCLUSION

Polyolefin (PP, PE and so on) and polyolefin rubber (EPDM, EPM) are important materials for industrial use because they are the most widely used polymers in the world. On the other hand, polymer–clay nanocomposites possesses excellent properties (high mechanical properties, high gas barrier properties, high thermal stabilities) with addition of a small amount of clay. Therefore, a development of

polyolefin and polyolefin rubber–clay nanocomposite has been desired for a long time. We have successfully developed these polyolefin and polyolefin rubbers clay nanocomposites using various methods. After our success, a lot of researchers have started to study in these field and a huge number of research articles have been published.[13–32] We expect that clay-based nanocomposite technology is grown into the universal method for high-performance materials from structural to functional ones extensively.

1 Usuki, A., Kojima, Y., Kawasumi, M., Okada, A., Kurauchi, T. & Kamigaito, O. Swelling behavior of montmorillonite cation exchange for omega-amino acids by ε-caprolactam. *J. Mat. Res.* **8,** 1174–1178 (1993).
2 Usuki, A., Kawasumi, M., Kojima, Y., Fukushima, Y., Okada, A., Kurauchi, T. & Kamigaito, O. Synthesis of nylon 6-clay hybrid. *J. Mat. Res.* **8,** 1179–1184 (1993).
3 Kojima, Y., Usuki, A., Kawasumi, M., Fukushima, Y., Okada, A., Kurauchi, T. & Kamigaito, O. Mechanical-properties of nylon 6-clay hybrid. *J. Mater. Res.* **8,** 1185–1189 (1993).
4 Usuki, A., Kato, M., Okada, A. & Kurauchi, T. Synthesis of polypropylene-clay hybrid. *J. Appl. Polym. Sci.* **63,** 137–139 (1997).
5 Kato, M., Usuki, A. & Okada, A. Synthesis of polypropylene oligomer—clay intercalation compounds. *J. Appl. Polym. Sci.* **66,** 1781–1785 (1997).
6 Hasegawa, N., Kawasumi, M., Kato, M., Usuki, A. & Okada, A. Preparation and mechanical properties of polypropylene-clay hybrids using a maleic anhydride-modified polypropylene oligomer. *J. Appl. Polym. Sci.* **67,** 87–92 (1998).
7 Hasegawa, N., Okamoto, H., Kato, M. & Usuki, A. Preparation and mechanical properties of polypropylene-clay hybrids based on modified polypropylene and organophilic clay. *J. Appl. Polym. Sci.* **78,** 1918–1922 (2000).
8 Kawasumi, M., Hasegawa, N., Kato, M., Usuki, A. & Okada, A. Preparation and mechanical properties of polypropylene-clay hybrids. *Macromolecules* **30,** 6333–6338 (1997).
9 Kato, M., Okamoto, H., Hasegawa, N., Tsukigase, A. & Usuki, A. Preparation and properties of polyethylene-clay hybrids. *Polym. Eng. Sci.* **43,** 1312–1316 (2003).
10 Nielsen, L. E. Models for the permeability of filled polymer systems. *J. Macromol. Sci. Chem.* **1,** 929–942 (1967).
11 Hasegawa, N., Okamoto, H. & Usuki, A. Preparation and properties of ethylene propylene rubber (EPR)-clay nanocomposites based on maleic-anhydride modified EPR and organophilic clay. *J. Appl. Polym. Sci.* **93,** 758–764 (2004).
12 Usuki, A., Tsukigase, A. & Kato, M. Preparation and properties of EPDM clay hybrids. *Polymer* **43,** 2185–2189 (2002).
13 Gilman, J. W., Jackson, C. L., Morgan, A. B., Harris, R., Manias, E., Giannelis, E. P., Wuthenow, M., Hilton, D. & Phillips, S. H. Flammability properties of polymer Layered-silicate nanocomposites. Polypropylene and polystyrene nanocomposites. *Chem. Mat.* **12,** 1866–1873 (2000).
14 Solomon, M. J., Almusallam, A. S., Seefeldt, K. F., Somwangthanaroj, A. & Varadan, P. Rheology of polypropylene/clay hybrid materials. *Macromolecules* **34,** 1864–1872 (2001).
15 Galgali, G., Ramesh, C. & Lele, A. A rheological study on the kinetics of hybrid formation in polypropylene nanocomposites. *Macromolecules* **34,** 852–858 (2001).
16 Nam, P. H., Maiti, P., Okamoto, M., Kotaka, T., Hasegawa, N. & Usuki, A. A hierarchical structure and properties of intercalated polypropylene/clay nanocomposites. *Polymer* **42,** 9633–9640 (2001).
17 Gopakumar, T. G., Lee, J. A., Kontopoulou, M. & Parent, J. S. Influence of clay exfoliation on the physical properties of montmorillonite/polyethylene composites. *Polymer* **43,** 5483–5491 (2002).
18 Reichert, P., Nitz, H., Klinke, S., Brandsch, R., Thomann, R. & Mulhaupt, R. Poly(propylene)/organoclay nanocomposite formation: influence of compatibilizer functionality and organoclay modification. *Macromol. Mater. Eng.* **275,** 8–17 (2000).
19 Liu, X. H. & Wu, Q. J. PP/clay nanocomposites prepared by grafting-melt intercalation. *Polymer* **42,** 10013–10019 (2001).
20 Morgan, A. B. & Gilman, J. W. Characterization of polymer-layered silicate (clay) nanocomposites by transmission electron microscopy and X-ray diffraction: a comparative study. *J. Appl. Polym. Sci.* **87,** 1329–1338 (2003).
21 Wang, K. H., Choi, M. H., Koo, C. M., Choi, Y. S. & Chung, I. J. Synthesis and characterization of maleated polyethylene/clay nanocomposites. *Polymer* **42,** 9819–9826 (2001).
22 Chow, W. S., Abu Bakar, A., Ishak, Z. A. M., Karger-Kocsis, J. & Ishiaku, U. S. Effect of maleic anhydride-grafted ethylene-propylene rubber on the mechanical, rheological and morphological. *Eur. Polym. J.* **41,** 687–696 (2005).
23 Chang, Y. W., Yang, Y. C., Ryu, S. & Nah, C. Preparation and properties of EPDM organomontmorillonite hybrid nanocomposites. *Polym. Int.* **51,** 319–324 (2002).
24 Zheng, H., Zhang, Y., Peng, Z. L. & Zhang, Y. X. Influence of clay modification on the structure and mechanical properties of EPDM/montmorillonite nanocomposites. *Polym. Test* **23,** 217–223 (2004).
25 Zheng, H., Zhang, Y., Peng, Z. L. & Zhang, Y. X. Influence of the clay modification and compatibilizer on the structure and mechanical properties of ethylenepropylene-diene rubber/montmorillonite composites. *J. Appl. Polym. Sci.* **92,** 638–646 (2004).
26 Wu, Y. P., Ma, Y., Wang, Y. Q. & Zhang, L. Q. Effects of characteristics of rubber, mixing and vulcanization on the structure and properties of rubber/clay nanocomposites by melt blending. *Macromol. Mater. Eng.* **289,** 890–894 (2004).
27 Gatos, K. G., Thomann, R. & Karger-Kocsis, J. Characteristics of ethylene propylene diene monomer rubber/organoclay nanocomposites resulting from different processing conditions and formulations. *Polym. Int.* **53,** 1191–1197 (2004).
28 Gatos, K. G. & Karger-Kocsis, J. Effects of primary and quaternary amine intercalants on the organoclay dispersion in a sulfur-cured EPDM rubber. *Polymer* **46,** 3069–3076 (2005).
29 Acharya, H., Pramanik, M., Srivastava, S. K. & Bhowmick, A. K. Synthesis and evaluation of high-performance ethylene-propylene-diene terpolymer/organoclay nanoscale composites. *J. Appl. Polym. Sci.* **93,** 2429–2436 (2004).
30 Morlat-Therias, S., Mailhot, B., Gardette, J. L., Da Silva, C., Haidar, B. & Vidal, A. Photooxidation of ethylene-propylene-diene/montmorillonite nanocomposites. *Polym. Degrad. Stabil.* **90,** 78–85 (2005).
31 Acharya, H., Srivastava, S. K. & Bhowmick, A. K. Synthesis of partially exfoliated EPDM/LDH nanocomposites by solution intercalation: structural characterization and properties. *Compos. Sci. Tech.* **67,** 2807–2816 (2007).
32 Naderi, G., Lafleur, P. G. & Dubois, C. Microstructure-properties correlations in dynamically vulcanized nanocomposite thermoplastic elastomers based on PP/EPDM. *Polym. Eng. Sci.* **47,** 207–217 (2007).

Makoto Kato was born in Aichi, Japan in 1959. He received his Bachelor and Master degrees in Engineering from Nagoya University in 1983 and 1985, respectively. He joined Toyota Central Research and Development Laboratories, Inc. (TCRDL) as a coating and a polymer scientist in 1985. He received his PhD degree from Nagoya University in 2005. He has now been working as a research manager in Coatings Laboratory in TCRDL. He received the outstanding technology award from the Society of Silicon Chemistry, Japan in 2007. His current research interests focus on coatings, coating materials, biopolymers and polymer nanocomposites.

Arimitsu Usuki was born in Aichi, Japan in 1955. He received his Bachelor and Master degrees in Engineering from Nagoya University in 1978 and 1980, respectively. He joined TCRDL as a polymer scientist in 1980. He received his PhD degree from Nagoya University in 1997. He has now been working as a director in TCRDL. He received the outstanding technology award from the Society of Silicon Chemistry, Japan in 2007. His current research interests focus on automotive materials.

Naoki Hasegawa was born in Aichi, Japan in 1965. He received his Bachelor and Master degrees in Engineering from Kyoto University in 1989 and 1991, respectively. He joined TCRDL in 1991. He received his PhD degree in Engineering from Kyoto University in 2005 on polymer–clay nanocomposites. He received the outstanding technology award from the Society of Silicon Chemistry, Japan in 2007. He has now been working as a research manager in Electrochemistry Division in TCRDL. His current research interests focus on fuel cells and their related materials.

Hirotaka Okamoto was born in Aichi, Japan in 1967. He received his Master and Doctor degrees in Engineering from Kyoto University in 1992 and 1995, respectively. He joined TCRDL as a polymer scientist in 1995. He has now been working as a senior researcher in Organic Material Laboratory in TCRDL. He received the best paper award from the Society of Rubber Industry, Japan in 2000 and the Nikkei green technology award in 2002. His current research interests focus on polymer blends and nanocomposite materials.

Masaya Kawasumi was born in Aichi, Japan in 1960. He received his Bachelor and Master degrees in Agriculture from Nagoya University in 1983 and 1985, respectively. He joined TCRDL as a polymer scientist in 1985. He received his PhD degree from Case Western Reserve University in Ohio, USA under the supervision of Professor Virgil Percec, in 1992. He has now been working as a fellow in Electrochemistry Division in TCRDL. He received the outstanding technology award from the Society of Silicon Chemistry, Japan in 2007. His current research interests focus on fuel cells, batteries and their related materials.